energies

MDPI

Article

Comparative and Sensitivity Analysis of Numerical Methods for the Discretization of Opaque Structures and Parameters of Glass Components for EN ISO 52016-1

Serena Summa *, Giada Remia and Costanzo Di Perna

Industrial Engineering and Mathematical Sciences Department, Università Politecnica Delle Marche, Via Brecce Bianche 1, 60131 Ancona, Italy; g.remia@pm.univpm.it (G.R.); c.diperna@univpm.it (C.D.P.)
* Correspondence: s.summa@pm.univpm.it

Abstract: The EN ISO 52016-1:2017 standard introduced a new methodology for the hourly calculation of energy needs that allows the study of the dynamic energy performance of buildings. In this study, a comparative analysis was carried out between two heat transfer models for opaque building elements: the one described in the new standard EN ISO 52016-1:2017 (Annex B) and that proposed by the Italian national annex (Annex A). The analysis, carried out on 1854 cases, showed better results for the heating period than for the cooling period, with a lower Root-Mean-Square Error and Coefficient of Variation of the Root-Mean-Square Error for the model proposed by the Italian National Annex. Increasing the performance of the building by decreasing the solar transmission coefficient of the glazed surfaces leads to a worse Root-Mean-Square Error of about 11%. In addition, a sensitivity analysis of the thermo-physical parameters of the opaque building components was carried out and an alternative method for the calculation of the solar transmission coefficient was evaluated. The latter was able to improve the Root-Mean-Square Error of summer solar gains by 46.7% compared to the method proposed by the standard.

Keywords: building energy performance; ISO 52016-1; building simulation; accuracy estimation; electro-thermal analogy of opaque component; solar transmission coefficient

Citation: Summa, S.; Remia, G.; Di Perna, C. Comparative and Sensitivity Analysis of Numerical Methods for the Discretization of Opaque Structures and Parameters of Glass Components for EN ISO 52016-1. *Energies* **2022**, *15*, 1030. https://doi.org/10.3390/en15031030

Academic Editors: Andrea Frazzica and Chi-Ming Lai

Received: 31 December 2021
Accepted: 19 January 2022
Published: 29 January 2022

1. Introduction

The necessity to reduce the energy demand of buildings by 80% (compared to 1990) by 2050 [1] and CO_2 emissions [2], has prompted the European Committee for Standardisation (CEN) to approve a package of new standards to support the implementation of the Energy Performance Building Directive (EPBD) [3]. In particular, EN ISO 52016-1:2017 [4] introduced a new methodology for the hourly calculation of energy needs for heating and cooling, that allows to investigate the dynamic energy performance of buildings. This standard shows great potential but currently there are not enough studies in the literature to validate its accuracy. Application studies used the standard to evaluate the summer performance of Trombe walls [5] or to assess the impact of highly massive envelope on the energy performance of a building [6]. In reference [7] the authors compare the energy requirements, obtained with the semi-stationary monthly method of EN ISO 13790, with the dynamic hourly method of the Standard and show discrepancies up to 100% for the winter period and up to 11% for the summer period. Congedo et al. [8] want to demonstrate that the hourly monitoring of the indoor operating temperature, according to EN ISO 52016, allows to univocally define the performance of the building, especially in terms of indoor comfort. Comparative studies, such as that of Ballarini et al. [9], argue that the main causes of deviation between the new hourly model and dynamic software, such as EnergyPlus, can be mainly attributed to usage of different surface heat transfer coefficients and a different modelling of the extra thermal radiation to the sky. Moreover, the work proposed by Zakula et al. [10,11] shows that the discrepancies between EN ISO 52016-1:2017

and Trnsys (albeit with acceptable CVRSME values), are mainly caused by three factors: (i) the use of constant values for the window transmittance (U_w), (ii) the use of constant values for the solar transmission coefficient (g_w) and (iii) minimally the calculation of heat transfer through opaque elements. Concerning the latter aspect, the work carried out by Mazzarella et al. [12] (incorporated in the Italian national annex of the standard), proposes an alternative method for the spatial discretization of the nodes of opaque structures based on the material and distribution of the effective layers. Analyses on individual walls have shown that this alternative method provides a more accurate approximation than the method proposed in the main text of the International Standard.

The purpose and novelty of this paper is to answer some problems that emerged from the previously mentioned studies and to expand the current knowledge of EN ISO 52016-1:2017 [4]. In fact, for the first time it was:

- tested the new method described in Annex A (Italian Annex) of EN ISO 52016-1:2017 [4];
- proposed a model capable of varying the g_{gl} at each time step (1 h), according to the orientation of the window and the angle of incidence of solar radiation;
- explored the effects of thermo-physical parameters of opaque surfaces on building energy needs through a sensitivity analysis of the Italian annex, the European annex and Trnsys.

In addition to identifying the application limits and problems of the standard, as already done in other works in the literature, this work proposes solutions that improve the hourly dynamic method of EN ISO 52016-1 [4], bringing the results closer to those obtained with Trnsys.

2. Methods

In order to identify the hourly energy demand for heating and cooling under different boundary conditions, three methods were compared. The following were used: (i) the calculation procedure defined in EN ISO 52016-1:2017 with European Annex [4] (later in the text referred to as Annex B), (ii) the calculation procedure defined in EN ISO 52016-1:2017 with Italian Annex [12] (later in the text referred to as Annex A) and (iii) the algorithm implemented in the energy modelling software TRNSYS [13].

2.1. EN ISO 52016-1:2017

The calculation algorithm defined by EN ISO 52016-1 [4] provides in output, for each thermal zone and for each hour, the values of parameters such as the internal air temperature, the average internal radiant temperature and the internal operating temperature useful to evaluate the internal comfort of the environments according to EN ISO 15251 [14]. In addition to temperatures, it also provides the energy needs for heating and cooling, which are essential for the energy assessment of the building. For each heated thermal zone and for each hourly time interval, the standard follows this procedure:

1. in absence of heating and cooling plant the internal operating temperature is evaluated; if this is between the heating and cooling set-point temperature, the system is not switched on and the output power is zero;
2. if the operating temperature is lower/upper than the heating/cooling set-point respectively, the power required by the system to guarantee the defined set-point temperature is calculated;
3. if the power of the system is sufficient, the set-point temperature is guaranteed;
4. if the power of the system is not sufficient, the set-point temperature is not reached;
5. the node temperatures of all the structures are determined according to the European or National Annex;
6. the effective energy load for heating and cooling is determined.

This is shown in Figure 1.

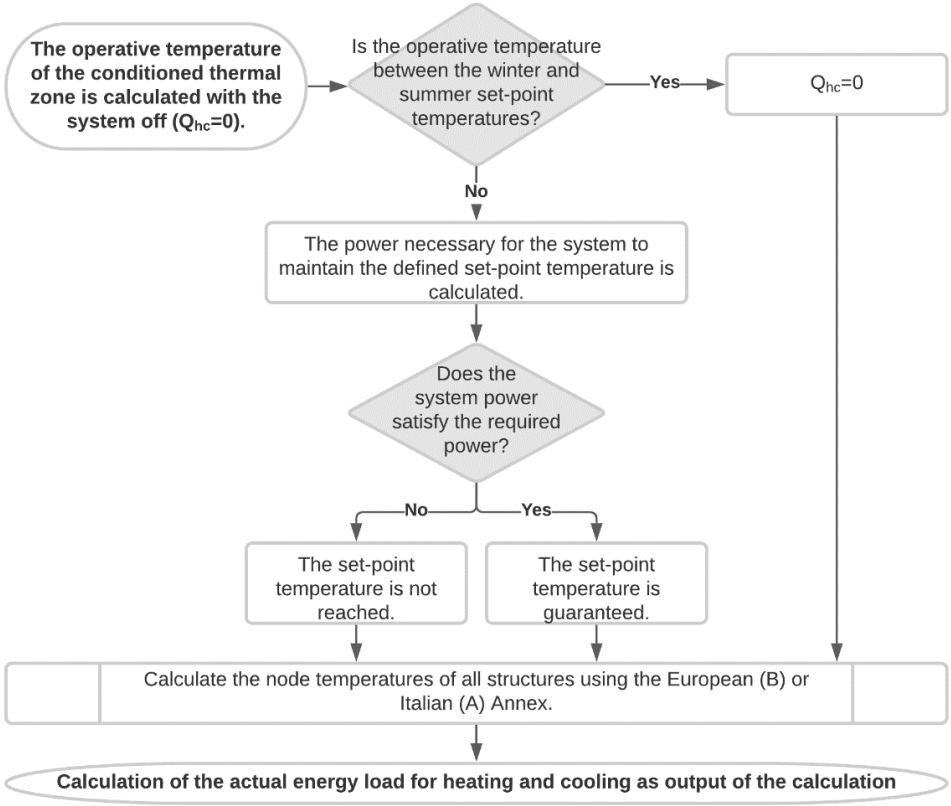

Figure 1. Flow chart of the calculation algorithm.

In order to determine the temperatures of the nodes of the structures, the calculation algorithm requires, for each time interval, the resolution of a system of energy balance equations carried out both for each thermal zone and for each individual building elements. The heat balance of the thermal zone provides, for each time interval, the evaluation of (i) the internal thermal capacity, (ii) the convective heat exchanges with the surface nodes of all structures, (iii) the heat exchange by ventilation, (iv) the heat exchange due to thermal bridges and, lastly, (v) the convective fractions of the total internal contributions, the solar contributions transmitted through the glass surfaces and the contributions due to the load of the heating/cooling plant. The thermal balances of building elements are evaluated by breaking down each building element (i.e., floors, walls, doors and windows) into a number of capacitive nodes and resistive layers. From the position of the node inside the opaque element, there are three different energy balances:

- the balance of the inside-facing node that considers the convective heat exchanges with the inside air, the conductive heat exchanges with the first node inside the opaque element, the heat exchanges by radiation with the surface nodes of all the structures delimiting the thermal zone, the eventual heat capacity associated with the surface node considered and the complementary quotas of the convective fractions of the total internal contributions, the solar contributions transmitted through the glass surfaces and the contributions due to the load of the heating/cooling system.
- the energy balances of the nodes inside the opaque element that consider the conductive thermal exchanges with adjacent nodes and any associated thermal capacities of the nodes.
- the balance of the outside-facing node, which considers convective heat exchanges with the outside air, radiation heat exchanges with the sky and solar contributions calculated as a function of the solar absorption coefficient, direct and diffuse solar radiation and any shading factor due to external obstacles.

The size of the matrix system is equal to the number of thermal zones plus the number of nodes of all building elements.

The method of EN ISO 52016 [15], based on the electro-thermal analogy, represents the thermo-physical characteristics of building structures with a resistive-capacitive circuit model where the mass is the accumulator (node), the transmittance is the resistive element (layer) and the heat flow is the current. The number of nodes of transparent elements is always 2, while the number of nodes of opaque elements differs according to the European Annex (Annex B) or Italian Annex (Annex A). The differences between the two Annexes are specified below.

2.1.1. European Annex

As shown in Figure 2, the opaque elements of EN ISO 52016-1:2017 are modelled with an RC network consisting of five nodes interconnected by four resistors.

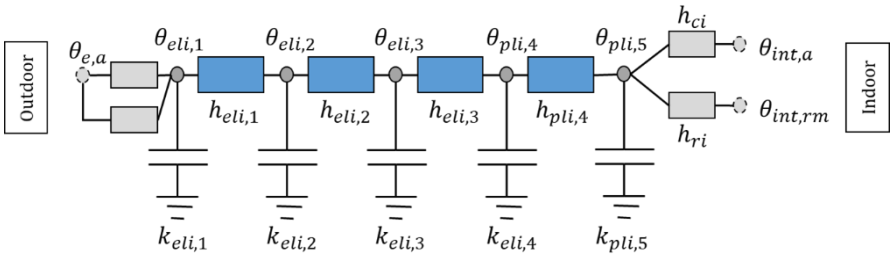

Figure 2. RC network of lumped parameters model proposed in EN ISO 52016-1.

Since the position of the nodes is independent of the number and the thermal-physical characteristics of each layer, the input parameters necessary for the method are the thermal resistance of the opaque element in m^2K/W and areal heat capacity of the opaque element in $J/(m^2K)$. The conductance between nodes pli and node pli-1 are fixed in function of the thermal resistance of the opaque element, as follows: heli;1 = heli; 4 = 6/Rce,eli and heli; 2 = heli; 3 = 3/Rce,eli. While the thermal capacity of the element (see Table 1) is divided to the nodes according to the position of the masses in the construction, namely internal (class I), external (class E), divided between inside and outside (class IE), equally distributed (class D) or inside concentrated (class M). The areal capacity value (κm,eli) is given in table B.14 of EN ISO 52016-1:2017 as a function of wall weight or if specified in the national annexes can be calculated.

Table 1. Values of the thermal capacities of the nodes as a function of the position of the mass, as defined in EN ISO 52016. Adapted from EN ISO 52016-1:2017.

Mass Position	$\kappa_{pl1,eli}$	$\kappa_{pl2,eli}$	$\kappa_{pl3,eli}$	$\kappa_{pl4,eli}$	$\kappa_{pl5,eli}$
I	0	0	0	0	$\kappa_{m,eli}$
E	$\kappa_{m,eli}$	0	0	0	0
IE	$\kappa_{m,eli}/2$	0	0	0	$\kappa_{m,eli}/2$
D	$\kappa_{m,eli}/8$	$\kappa_{m,eli}/4$	$\kappa_{m,eli}/4$	$\kappa_{m,eli}/4$	$\kappa_{m,eli}/8$
M	0	0	$\kappa_{m,eli}$	0	0

2.1.2. Italian Annex

Concerning the Italian model (Annex A), instead, the number of nodes is not pre-defined but is calculated for each *j*-th real layer of the building component, obtaining a number of capacitive nodes equal to the result of the following expression:

$$N_{cn,j} = \max\{1; (Fo_{ref}/Fo_j)^{1/2} + 0.999999\} \quad (1)$$

where:

Fo_{ref} is the reference Fourier number set to 0.5 [12]

Fo_j is the Fourier number of the *j*-th layer, calculated as $Fo_j = \Delta t \cdots \lambda/(\rho_j \cdots c_j \cdots d_j^2)$ [15]

with:

ρ_j: density of the material of the *j*-th layer of the building element (kg/m^3)
c_j: thermal capacity of the *j*-th layer of the building element (J/(kg·K))
d_j: thickness of the *j*-th layer of the building element (m)

Once identified the number of nodes in each *j*-th layer, the internode conductive resistances are assigned using the real thermal conductivity of the material and its relative layer thickness, as shown by Mazzarella et al. [12].

2.2. Trnsys

TRaNsient SYstems Simulation [13] is the most popular calculation code used by researchers and engineers for the dynamic simulation of complex systems such as building-plant systems. As in this case study, the simulation of a joint building-plant system requires two Trnsys interfaces: SimulationStudio and TRNBuild. Simulation Studio is a virtual environment that allows the study of physical phenomena through blocks called "Type". Among the various types required, "Type 56-Multizone Building" is the one that enables a multi-zone building to be modelled through the interface called TRNBuild. TRNBuild defines all the thermal zones that compose the building, the opaque and transparent elements, the thermophysical characteristics of the materials, the use profiles of the plants and all the input and output variables necessary to establish the connections between the model and the Simulation Studio environment. Figure 3 shows the diagram of the models used for our simulations. The external temperatures, relative humidity and solar radiation used for the two previous methods are given as input.

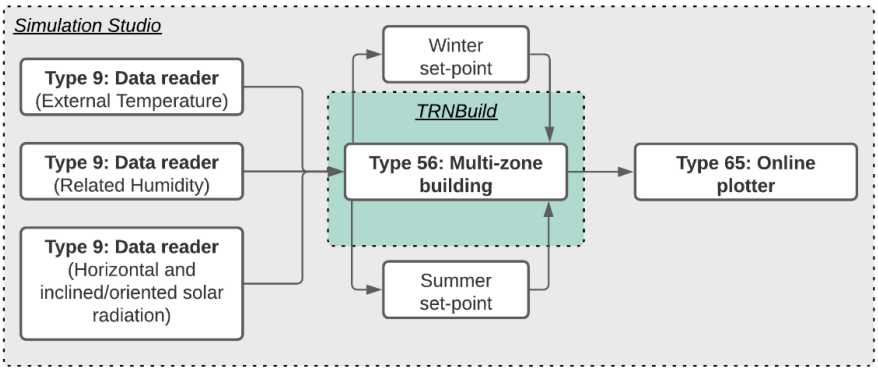

Figure 3. Model flowchart in Trnsys.

3. Case Studies

The study includes three different types of analysis (see Figure 4): the first aims to validate Annex A and Annex B of ISO 52016-1:2017 [4], the second aims to evaluate the response of the Standard to impulsive loads (solar radiation) through the variation of the solar transmission coefficient g_{gl} and the third aims to evaluate the impact of the thermo-physical parameters of opaque walls on the calculation of energy needs. In the second analysis, an algorithm is also tested which allows the calculation of solar transmission coefficient as a function of the window orientation and the angle of incidence of solar radiation [16].

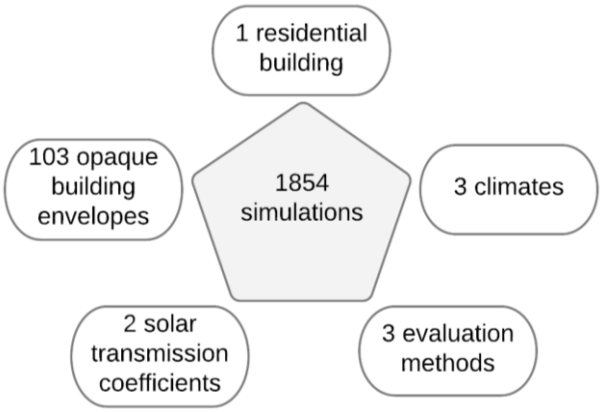

Figure 4. Overview of case studies: Evaluation of 3 heat transfer models for buildings with different thermal inertia and different solar transmission coefficients.

3.1. Geometry and Zoning

The residential case study analyzed (see Figure 5) is two floors building with a bathroom, a storage room, a kitchen and a living room on the ground floor, and two single rooms, a double room, a bathroom and a hallway on the first floor. EN ISO 52016-1 provides general guidelines for zoning buildings, suggesting that all adjacent spaces in the same category should be grouped together in a single thermal zone. Despite these indications many studies collected by Shin et al. [17] show that it is appropriate to divide the space into different thermal zones according to solar loads, orientation, occupancy and air conditioning schedule. Therefore, each room of the building was defined as a different thermal zone. Only the stairwell, unlike the other zones, is classified as an unheated thermal zone. The geometric characteristics of each thermal zone, i.e., the useful surface area (A_{floor}), the internal volume (V), the average internal height (h_{avg}) and the window area (A_{window}), are shown in Table 2.

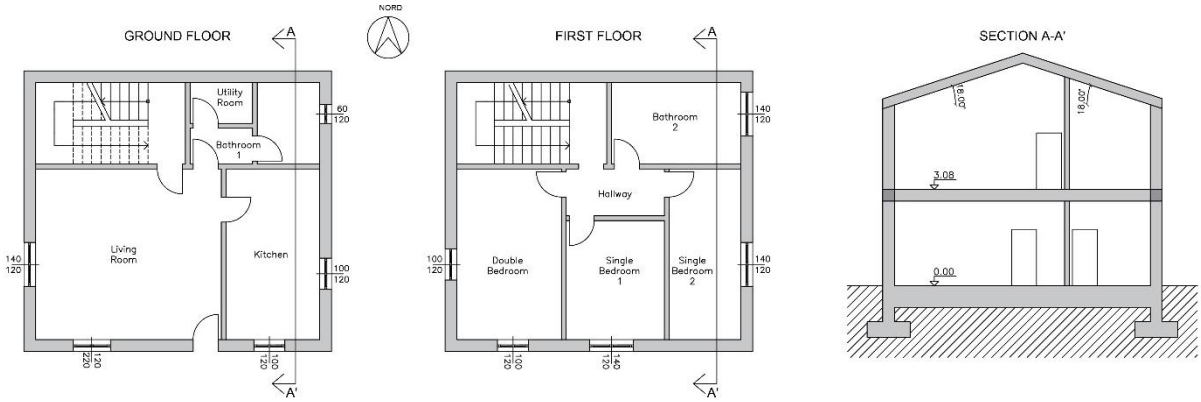

Figure 5. Plan view of the ground floor, first floor and section of the building model.

Table 2. Geometrical characteristics of thermal zones.

Room	A_{floor}	V	h_{avg}	A_{window}
-	m^2	m^3	m	m^2
Bathroom 1	7.50	20.25	2.70	0.41
Utility Room	2.60	7.02	2.70	0.00
Kitchen	16.35	44.15	2.70	1.64
Living Room	32.43	87.55	2.70	3.25
Bathroom 2	10.79	33.69	3.12	1.22
Hallway	4.73	18.11	3.83	0.00
Single Bedroom 1	11.97	39.71	3.32	1.22
Single Bedroom 2	12.54	43.58	3.48	1.22
Double Bedroom	18.26	63.47	3.48	1.64
Stairwell	12.48	72.66	5.82	0.00

3.2. Opaque Surfaces

In order to evaluate the effect of the thermophysical characteristics of the opaque vertical envelope and to significantly compare the various simulations, it was decided to keep some opaque structures constant, such as: ground slab, inter-floor slab, roof and internal walls. In addition to the thermo-physical characteristics of the listed structures, Table 3 also reports information on the distribution of mass within the opaque element, which is a necessary information for the application of the European method of EN ISO 52016-1:2017 standard [4].

Table 3. Thermo-physical characteristics of fixed structures. I: mass concentrated on the internal side. D: distributed mass.

Building Element	Distribution of Mass	U	M_s	Y_{IE}	fa	φ	κ_j
-	-	$W/(m^2K)$	kg/m^2	$W/(m^2K)$	-	h	$kJ/(m^2K)$
Roof	I	0.264	401.60	0.061	0.230	7.66	91.41
Ground Floor	D	0.353	1369.40	0.010	0.028	18.08	62.15
Interior Floor	D	0.354	403.80	0.039	0.111	12.28	52.20
Interior Walls	D	1.125	111.60	0.673	0.598	6.18	50.99

One hundred and three different vertical opaque envelopes were simulated, each characterized by different values of thermal transmittance, surface mass, periodic thermal transmittance and internal areal heat capacity. Among these walls, according to the classification reported in the Standard, 16 have a mass divided between internal and external (EI), 23 have a concentrated mass on the external side (E), 24 have a concentrated mass on the internal side (I) and 40 have a distributed mass (D). The 103 walls studied include the following technological solutions: single-layer masonry in thermo-brick, multi-layer masonry with cavity insulation, masonry with external insulation, masonry with internal insulation, light wood and plaster fiber walls. Table 4 shows the ranges of the thermo-physical parameters of the analyzed walls, while in Table A1 they are specified in detail.

Table 4. Range of thermo-physical parameters of the walls analyzed.

Parameter	Min	Max
U $[W/(m^2K)]$	0.163	0.598
M_s $[kg/m^2]$	18.60	444.15
Y_{IE} $[W/(m^2K)]$	0.001	0.339
f_a [-]	0.003	0.953
φ [h]	2.05	32.77
κ_j $[kJ/(m^2K)]$	21.56	50.13

3.3. Transparent Surfaces

The glazed structures were sized (see Table 5) taking the minimum surface value obtained between the calculation of the daylight factor (at least 2%) and the calculation of 1/8 of the usable floor area of each thermal zone. These two limits are given in the Italian Ministerial Decree of 05/07/1975 [18] while the calculation of the daylight factor was carried out according to the UNI 10840:2007 standard [19]. In order to evaluate the management of impulsive loads by the calculation algorithm reported in EN ISO 52016-1:2017 [4], it was decided to consider two solar transmission coefficients: $g_{gl,n}$ = 0.77 (case study 1) and $g_{gl,n}$ = 0.34 (case study 2). In no case fixed or movable shading systems are considered, therefore only the influence of g_{gl} on the calculation of the energy demand is evaluated.

Table 5. Thermal transmittance and solar transmission coefficient of windows used.

b_{window}	h_{window}	$U_{case\ study\ 1=case\ study\ 2}$	$g_{gl,n,case\ study\ 1}$	$g_{gl,n,case\ study\ 2}$
m	**m**	**W/(m^{2}K)**	**-**	**-**
0.60	1.20	2.00	0.77	0.34
1.00	1.20	2.19	0.77	0.34
1.40	1.20	2.27	0.77	0.34
1.20	2.20	2.34	0.77	0.34

Considering an average thickness of all the walls used of 36 cm, the ratio of glazed to opaque surfaces is: 0% in the North, 11.1% in the South, 8.6% in the East and 4.7% in the West.

3.4. Climate and Other Assumptions

The energy needs for heating and cooling were calculated for a typical meteorological year for three Italian climatic zones identified in DPR 412/1993 [20]: Milan, Rome and Palermo. Hourly climatic data defined in national databases were used for each location (see Table 6).

Table 6. Outdoor temperature (min, max and average), horizontal solar radiation (max and average) and heating degree days of the three considered locations.

Site	$\theta_{e,min}$	$\theta_{e,max}$	$\theta_{e,avg}$	$I_{H,max}$	$I_{H,avg}$	HDD	Köppen-Classification
-	**°C**	**°C**	**°C**	**W/m^2**	**W/m^2**	**-**	**-**
Milan	−1.80	33.70	14.29	1000.00	150.27	2274	Cfa
Rome	−0.12	37.38	16.72	968.90	180.81	1630	Csa
Palermo	0.21	36.91	18.99	986.10	181.08	1089	Csa

For the calculation of direct and diffuse radiation on horizontal and inclined/oriented surfaces, EN ISO 52016-1:2017 [4] refers to EN ISO 52010-1:2017 [21], which allows the use of different calculation models. In this study, the calculation method proposed in [22] is used. This method, in a comparative analysis on five European cities and for four calculation algorithms (Trnsys [13], Meteonorm [23], EN ISO 52010-1:2017 [21] and the proposed method) returns values closer to those calculated with Trnsys. The UNI-TS 11300-1: 2014 [24] standard was used to determine the internal gains, where, for useful surfaces of residential buildings greater than 120 m^2, the value of the internal contributions is set at 450 W. Dividing this value by the useful surface of each thermal zone, the thermal inputs for each room are obtained. These contributions are considered constant throughout the calculation period. Moreover, a constant natural ventilation was considered, using an air exchange rate of 0.50 1/h.

For the winter season the set-point temperature was set at 20 °C, and for the summer season at 26 °C. The switch-on profile of the systems is constant for each location. The heating system is switched on for 12 h a day, from 7:00 A.M. to 11:00 A.M. and from 4:00 P.M. to 10:00 P.M., while the cooling system is switched on for 8 h a day, from 11:00 A.M. to 6:00 P.M., both from 1 January to 31 December with infinite power.

In this study, thermal bridges and shading caused by external elements or curtains were not considered, while the heat exchange with the ground is considered adiabatic. In particular, the choice not to consider shading has allowed to highlight better the inci-dence of the total solar energy transmission coefficient (g_{gl}) on the method of EN ISO 52016, avoiding having energy requirements "forcedly" aligned with Trnsys due to absent solar gains.

4. Results and Discussion

The following metrics were used to assess the accuracy of the Standard (European and Italian annexes) compared to Trnsys:

CV(RMSE) (Coefficient of Variation of the Root-Mean-Square Error) is used to calibrate models in measured building performance. This metric indicates instability in the observed relationship between variables in the baseline period. It is the coefficient of the variation of the predicted input series relative to the observed input series (Trnsys) [25].

According to ASHRAE guideline 14 [26], an hourly energy model is considered accurate if the CV(RMSE) value is less than 30%.

$$\mathrm{CV(RMSE)} = \sqrt{\left(\sum_{i=1}^{n}(T_i - M_i)^2/n\right)} / \overline{T} \cdots 100\ [\%] \tag{2}$$

where T_i and M_i are respectively the hourly data from Trnsys and the hourly data from the other methods used, n is the number of hours in which Trnsys gives a non-zero value in the considered interval (heating or cooling hours) and $\overline{T}$ is the average of the hourly data from Trnsys.

RMSE (Root-Mean-Square Error) is the standard deviation of the residuals (prediction errors). The effect of each error on RMSE is proportional to the size of the squared error; thus, larger errors have a disproportionately large effect on RMSE. Consequently, RMSE is sensitive to outliers [27].

$$\mathrm{RMSE} = \sqrt{\left(\sum_{i=1}^{n}(T_i - M_i)^2/n\right)}\ [\mathrm{kWh\ or\ ^\circ C}] \tag{3}$$

4.1. Accuracy of the Standard (European and Italian Annex)

Analyzing as a case study the building defined in Section 3, with g_{gl} = Fw x $g_{gl,n}$ = 0.9 × 0.77 = 0.693, the results obtained with Annex B and Italian Annex A are compared with Trnsys. Considering the maximum annual heating, cooling and total demand of 61.4 kWh/m^2, 34.1 kWh/m^2 and 75.8 kWh/m^2, and a minimum annual heating, cooling and total demand of 2.9 kWh/m^2, 11.4 kWh/m^2 and 30.9 kWh/m^2, the building in all its configurations and locations can be categorized as a low energy building [28]. For each city in the case study, the RMSE is extremely small. Regarding heating, both methods show variations of less than 1 kWh, and for cooling variations of less than 2 kWh. Furthermore, unlike heating where the RMSE seems to vary as a function of the annual hourly needs, in the cooling phase the error seems to be less dependent on the energy needs (see Figure 6). While the absolute error RMSE is low, the relative error CV(RMSE) is often above the ASHRAE limit of 30%. However, it should be noted that this is predominantly caused by the low energy needs of the analyzed solutions, which affect the denominator of Equation (2), increasing the relative error. From Figure 7 and Table 7, in the heating period, the error increases to 98% for the city with the warmest climate and decreases to 23% for the city with the coldest climate. Conversely, in the cooling period the error reaches a maximum of 150% for the coldest city and a minimum of 35% for the warmest city. Only in the winter

phase there are cases where the CV(RMSE) is less than 30%, precisely 16 cases (5.2%) for Annex B and 45 cases (14.6%) for Annex A. Although these percentages are low, considering the small number of kWh/m^2 consumed by the building, they are consistent with those obtained from the Zakula et al. study [11].

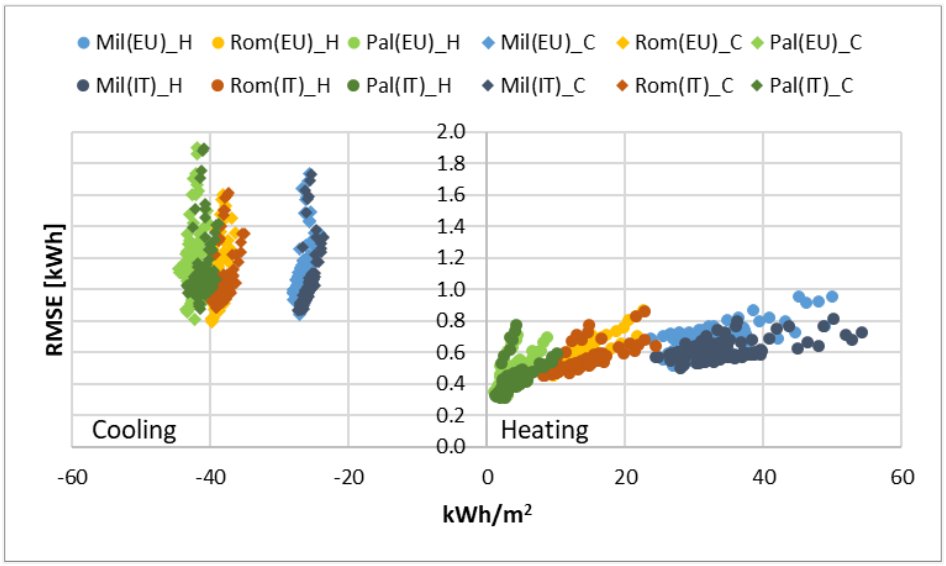

Figure 6. RMSE for heating and cooling needs, for all climates of the case study and for both methods (EU: Annex B, IT: Annex A): Case study with $g_{gl,n}$ = 0.77.

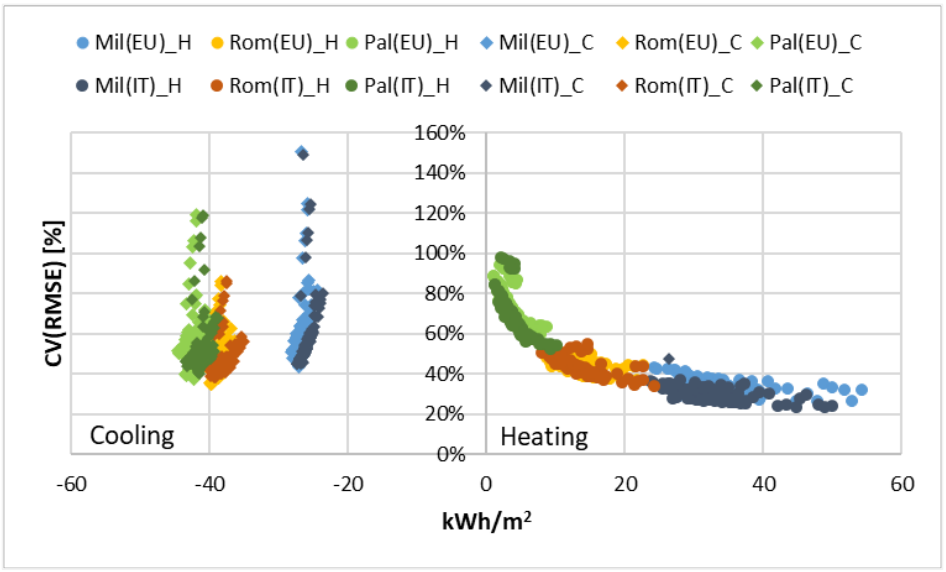

Figure 7. CV(RMSE) for heating and cooling needs, for all climates of the case study and for both methods (EU: Annex B, IT: Annex A): Case study with $g_{gl,n}$ = 0.77.

Table 7. Minimum, maximum, average and standard deviation value of CV(RMSE) and the RMSE of both methods of EN ISO 52016 (Annex A and Annex B). Case study with $g_{gl,n}$ = 0.77. The gray cells show the best percentages.

	Heating				Cooling			
	CV(RMSE) [%]		RMSE [kWh]		CV(RMSE) [%]		RMSE [kWh]	
	EU	IT	EU	IT	EU	IT	EU	IT
Min	26.2%	23.4%	0.32	0.31	34.6%	38.3%	0.80	0.87
Max	94.0%	98.0%	0.95	0.86	150.5%	149.0%	1.90	1.90
Avg	51.8%	48.4%	0.57	0.53	56.4%	53.3%	1.14	1.07
Dev.St.	18.6%	18.2%	0.12	0.11	14.9%	14.8%	0.19	0.18

In order to evaluate the differences in terms of internal temperatures and surface temperatures, we studied four different envelope configurations on a single thermal zone of the building. Taking the living room, that is the largest room and with the most glazed area, as the reference thermal zone (see Figure 8) we compared the internal temperatures and surface temperatures (points 1 to 10) of four layers with the same thermal transmittance but different mass positions (see Table 8). Walls 21, 75 and 87 (see Table 8) have respectively distributed mass, internal mass (external insulation) and external mass (internal insulation), while 44 is a low surface mass wall. RMSE is calculated between the temperatures obtained from Trnsys and those obtained from models described in the European and Italian annexes.

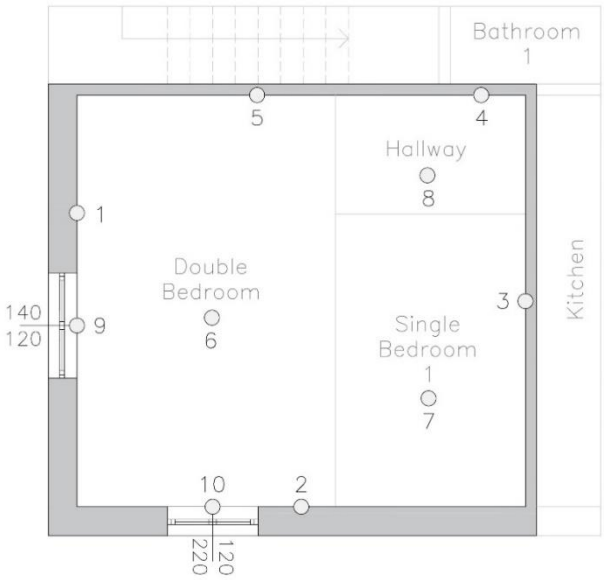

Figure 8. Indication of the points on which the surface temperatures of the living room are calculated.

Table 8. Selected structures, among those analyzed, with similar transmittance but different surface mass and mass distribution.

N.	Distribution of Mass	U	M_s	Y_{IE}	f_a	φ	κ_j
-	-	W/(m^{2}K)	kg/m^2	W/(m^{2}K)	-	h	kJ/(m^{2}K)
21	D	0.23	432	0.001	0.005	5.93	39.57
75	I	0.23	405	0.001	0.005	26.85	41.52
87	E	0.23	405	0.001	0.006	2.53	22.33
44	IE	0.23	21	0.192	0.888	3.81	34.26

The results in Figure 9, show that the use of Annex B leads to a greater error in terms of temperatures than the use of Annex A. In addition, it is important to note that the surface

temperatures of the external walls (1 and 2) calculated with Annex A have an approximately constant error (about 0.4 °C) for all four stratigraphies analyzed, when compared to Trnsys. In contrast, for annex B the error seems to vary according to the position of the mass inside the wall; obtaining the worst result for wall 87, that is characterized by external mass and internal insulation. This error affects the entire thermal zone by modifying the surface temperatures of the internal walls (3, 4 and 5) and the floor (6, 7 and 8) (see Figure 9). With regard to the operative, air and average radiant temperatures, the smallest error is obtained with Annex A.

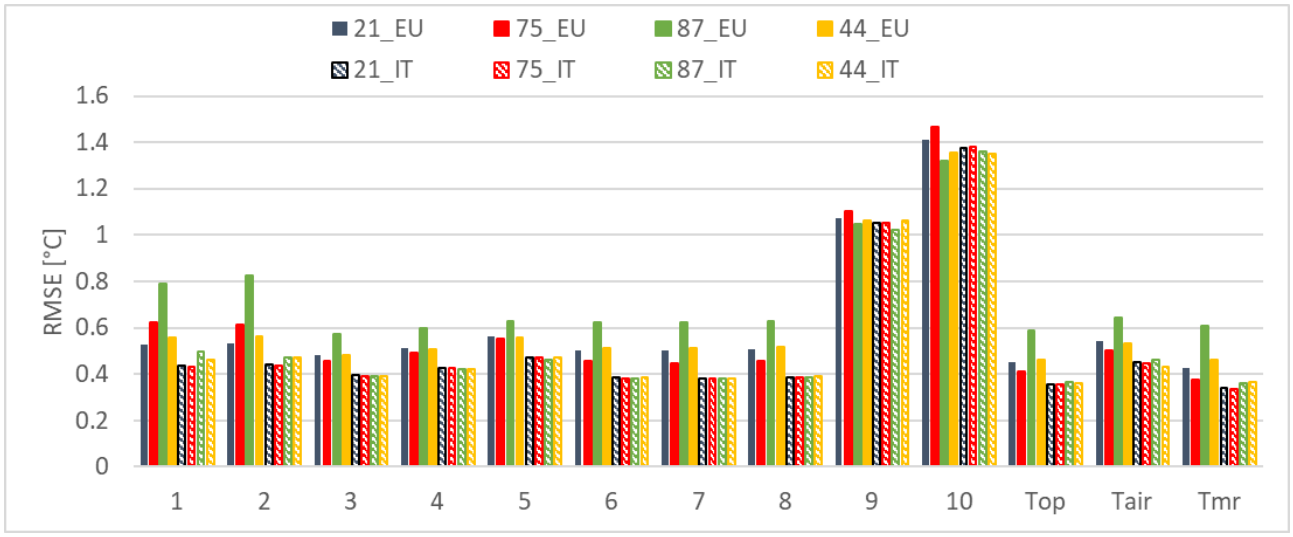

Figure 9. RMSE [°C] calculated for indoor and surface temperatures in the living room. (EU: Annex B, IT: Annex A).

4.2. Impact of the Solar Transmission Coefficient (ggl) on the Calculation of Energy Needs

Considering as case study the building defined in Section 3, with $g_{gl} = Fw \times {}_{gl,n} = 0.9 \times 0.34 = 0.306$, the results obtained with Annex B and Italian Annex A are compared with Trnsys. In this configuration, the maximum annual heating, cooling and total demand is 72.3 kWh/m^2, 14.3 kWh/m^2 and 76.8 kWh/m^2 and the minimum annual heating, cooling and total demand is 9.1 kWh/m^2, 2.2 kWh/m^2 and 22.5 kWh/m^2. Decreasing the solar transmission coefficient by 44% (from 0.77 to 0.34), leads to an increase in the heating demand and a decrease in the cooling demand (see Table 9). For all three climates, however, total energy demand decreases by 3.7%, 16.4% and 28.4% for Milan, Rome and Palermo, respectively.

Table 9. Average percentage difference and average energy difference between the case study with $g_{gl,n} = 0.77$ and $g_{gl,n} = 0.34$. $\Delta\varphi\% = (\varphi\_g_{gl},0.77 - \varphi\_g_{gl},0.34)/ \varphi\_g_{gl},0.77$. $\Delta kWh = (\varphi\_g_{gl},0.77 - \varphi\_g_{gl},0.34)$.

	Average Percentage Difference				**Average Energy Difference**		
	Δφ,h	**Δφ,c**	**Δφ,tot**		**Δφ,h**	**Δφ,c**	**Δφ,tot**
	[%]	**[%]**	**[%]**		**[kWh]**	**[kWh]**	**[kWh]**
Milan	−26.4%	68.3%	3.7%	Milan	−1193.0	1427.5	234.5
Rome	−61.2%	61.0%	16.4%	Rome	−1191.4	2069.5	878.1
Palermo	−126.0%	59.3%	28.4%	Palermo	−876.9	2106.0	1229.2

As in the case study with $g_{gl,n} = 0.77$, the RMSE is extremely small (see Figure 10). For heating, both methods show variations of less than 1 kWh, while for cooling the variations are greater than in the previous case study but still not more than 2.2 kWh. While the

absolute error (RMSE) is low, the relative error CV(RMSE) is often above the ASHRAE limit of 30%. As already mentioned, this is mainly due to the low energy requirements of the analyzed solutions, which affect the denominator of Equation (2), increasing the relative error. In fact, from Figure 11, during the heating phase, the error increases to 71% for the city with the warmest climate and decreases to 24% for the city with the coldest climate. Conversely, in the cooling phase the error reaches a maximum of 366% for the coldest city and a minimum of 62% for the warmest city. Only in winter some cases are characterized by the CV(RMSE) smaller than 30%, precisely 51 cases (16.5%) for Annex B and 81 cases (26.2%) for Annex A. With a lower solar transmittance coefficient, hence less incoming solar contributions, both models seem to perform better in terms of CV(RMSE) in the winter period, but only for the cooler city, while in the summer period no case satisfies the ASHRAE limit of 30%.

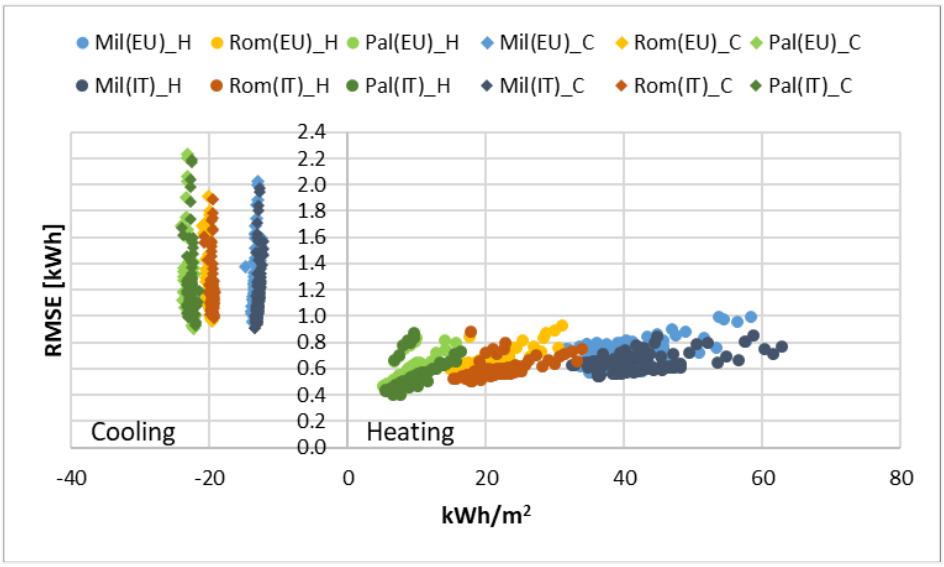

Figure 10. RMSE for heating and cooling needs, for all climates of the case study and for both methods (EU: Annex B, IT: Annex A): Case study with $g_{gl,n}$ = 0.34.

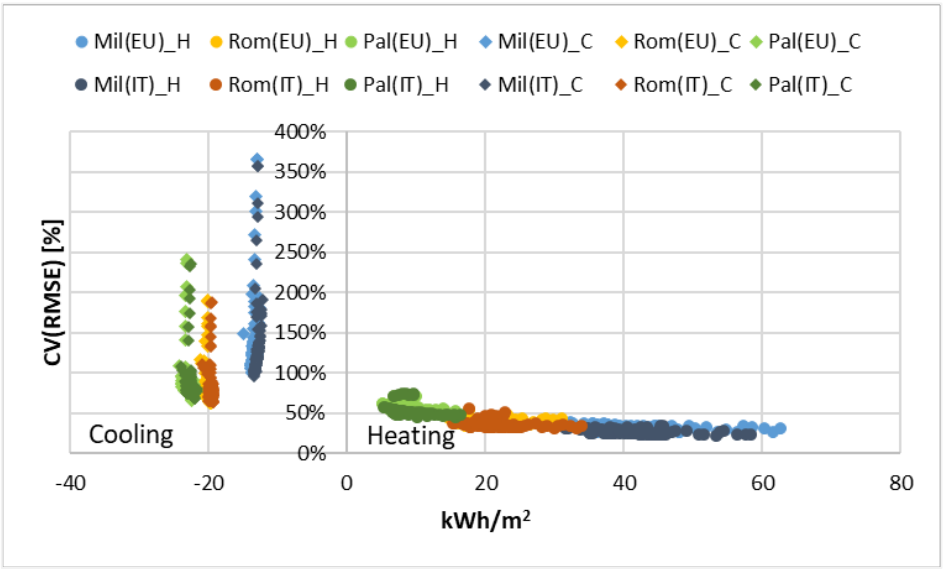

Figure 11. CV(RMSE) for heating and cooling needs, for all climates of the case study and for both methods (EU: Annex B, IT: Annex A): Case study with $g_{gl,n}$ = 0.34.

Comparing the two methods, from Table 10, the variable node method described in the Italian Annex A is closer to the results reported by Trnsys. Despite the greater number of structures that verify the relative error of 30%, decreasing the $g_{gl,n}$ leads to a worse RMSE absolute error than the case study with $g_{gl,n}$ = 0.77. In fact, in the winter season the average error is 12.9% and 11.6% worse for the method described in Annex B and Annex A respectively, while in the summer season it is 9.3% and 11.7% worse.

Table 10. Minimum, maximum, average and standard deviation value of CV(RMSE) and the RMSE of both methods of EN ISO 52016 (Annex A and Annex B). Case study with $g_{gl,n}$ = 0.34. The gray cells show the best percentages.

	Heating				Cooling			
	CV(RMSE) [%]		RMSE [kWh]		CV(RMSE) [%]		RMSE [kWh]	
	EU	IT	EU	IT	EU	IT	EU	IT
Min	24.1%	22.4%	0.41	0.40	62.0%	63.1%	0.91	0.91
Max	70.7%	74.5%	0.99	0.88	366.0%	356.6%	2.23	2.19
Avg	41.6%	38.5%	0.64	0.59	106.4%	102.6%	1.24	1.20
Dev.St.	11.0%	11.3%	0.11	0.09	43.4%	42.2%	0.23	0.23

Improved Calculation of the Total Solar Energy Transmission Coefficient (g_{gl})

As pointed out by Zakula et al. [10,11], while TRNSYS uses a relatively complex mathematical model for the calculation of the total solar energy transmission coefficient (g_{gl}) of the window, ISO 52016-1 uses very simplified correction factors (i.e., F_w = 0.9), although it considers the angle of incidence of solar radiation. This difference between the two calculation methods inevitably leads to the estimation of different solar contributions and energy needs, especially for the summer period. For this reason, in this analysis the algorithm of Karlsson et al. [16], also reported in the Italian National Annex, is tested, which allows to calculate the g_{gl} coefficient as a function of a variable F_w coefficient:

$$F_w = (F_{w,dif} \cdot I_{sol,dif,t} + F_{w,dir} \cdot I_{sol,dir,t} \cdot F_{sh,obst,t}) / (I_{sol,dif,t} + I_{sol,dir,t} \cdot F_{sh,obst,t}) \quad (4)$$

where $F_{w,dir}$ is the correction factor for direct radiation, $F_{w,dif}$ is the correction factor for diffuse radiation equal to 0.8, $I_{sol,dir,t}$ e $I_{sol,dif,t}$ is the direct and diffuse solar radiation incident on the glazed surface and $F_{sh,obst,t}$ is the shading reduction factor for external obstacles calculated in accordance with Annex E.

$$F_{w,dir} = 1–8 \cdots (\vartheta_{sol,t}/90)^{5.2+0.7q} - (0.25/q) \cdots (\vartheta_{sol,t}/90)^2 + (7+(0.25)/q) \cdots (\vartheta_{sol,t}/90)^{[(5.26+0.06p)+(0.73+0.04p)q]} \quad (5)$$

where $\vartheta_{sol,t}$ is the angle of incidence of direct solar radiation in degrees, p is the number of glass panels and q is the coefficient indicating the type of glass coating. The solar loads of the living room are calculated using the F_w coefficient of 0.9 (as suggested by Standars) and the variable F_w coefficient as shown in Equations (3) and (4); these loads are then compared with those of Trnsys.

From this analysis we observe that the variable F_w method allows summer solar loads to be more closely aligned with Trnsys loads, but the problem persists in the winter phase. The annual CV(RMSE) calculated for the method with $g_{gl,cost}$ and $g_{gl,var}$ is 33.54% and 28.95%, respectively. In particular, as can be observed in Table 11, in spring and summer the difference between the two CV(RMSE) is about 14% and between the two RMSE is about 40%, with the best results obtained for the proposed method ($g_{gl,var}$). In autumn and winter, the difference between the two CV(RMSE) is about 7% and between the two RMSE is less than 20%, with the best results obtained for the method with $g_{gl,cost}$. Despite the fact that in the cold seasons the proposed method seems to perform worse, the solar gains being lower than in the summer, have less impact on the heating needs. Conversely, as already observed in Sections 4.1 and 4.2, the error obtained on the calculation of the cooling

requirement is extremely greater than that of heating and, as emerges in the literature, is mainly caused by solar loads [29–32].

Table 11. Seasonal CV(RMSE) [%] and RMSE [kWh] calculated for the $g_{gl,cost}$ and $g_{gl,var}$ method.

	Spring		Summer		Autumn		Winter	
	21/03–21/06		22/06–22/09		23/09–21/12		22/12–20/03	
	CV(RMSE)	RMSE	CV(RMSE)	RMSE	CV(RMSE)	RMSE	CV(RMSE)	RMSE
$g_{gl,cost}$	33.29%	73.97	32.05%	76.78	33.59%	62.05	34.99%	58.47
$g_{gl,var}$	19.20%	42.66	17.26%	41.35	39.62%	73.21	43.10%	72.03

Thus, implementing the Karlsson et al. method [16] within the general algorithm of EN ISO 52016-1 [4] will allow the estimation of more accurate solar loads and consequently more precise summer energy demand.

4.3. Sensitivity Analysis of the Thermophysical Parameters of Opaque Walls on the Calculation of Energy Needs

Performing a sensitivity analysis is important in order to check the robustness of the conclusions of a study. This analysis allows to examine how the output results of the models used (i.e., heating or cooling energy needs) are influenced by the values of the input variables (i.e., the thermophysical parameters of the opaque elements).

Using the "Weight by Correlation" operator of the RapidMiner Studio software [33], the absolute values of the attribute weights (i.e., thermophysical parameters of opaque elements) were calculated with respect to the label attribute (i.e., heating or cooling energy needs). Values close to 1 will indicate a high correlation between the parameters, while values close to zero will indicate a low correlation. The weights obtained from the analysis of the models described in Annex A and B of EN ISO 52016-1 were compared with those obtained with the Trnsys software.

The dataset was divided by city and by case study ($g_{gl,n}$ = 0.77 and $g_{gl,n}$ = 0.34) and 6 different analyses were conducted. The specific values of the weights calculated by correlation are given in Appendix B of this manuscript.

In the heating season, for both g_{gl} configurations (see Figures 12 and 13) and for all calculation models (Annex A, Annex B and Trnsys), the stationary thermal transmittance (U) is the most important parameter. The periodic thermal transmittance (Yie), the phase shift (phi), the total thermal capacity (Ctot), the surface mass (Ms), the attenuation (fa) and lastly the internal heat capacity (ki) follow in descending order. This means that the different models are well aligned during heating.

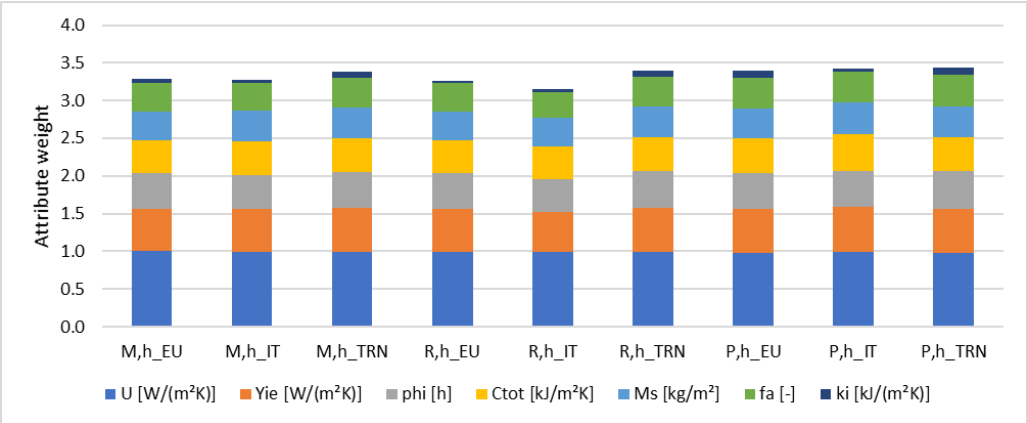

Figure 12. Weight analysis of the thermo-physical attributes of opaque structures, for the winter period and with $g_{gl,n}$ = 0.77.

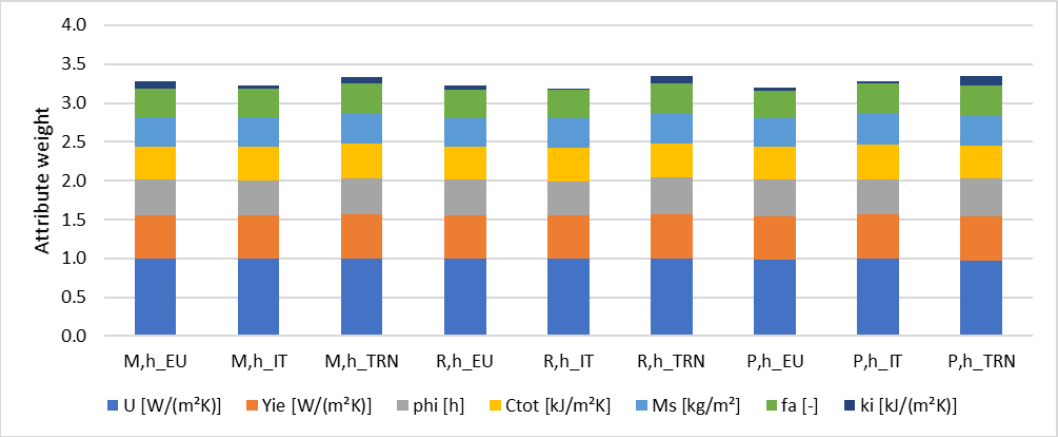

Figure 13. Weight analysis of the thermo-physical attributes of opaque structures, for the winter period and with $g_{gl,n}$ = 0.34.

In the cooling season, the weights of the attributes turn out to be very variable for the different methods and case studies. In Figure 14, for the case study with $g_{gl,n}$ = 0.77, the thermal transmittance is still the most important attribute, although with a weight of 17.4% lower than the winter one. Then, for Trnsys, in descending order, the phase shift (phi), the periodic thermal transmittance (Yie), the internal heat capacity (ki), the total heat capacity (Ctot), the surface mass (Ms) and finally the attenuation (fa) follow. Although there is a similarity in terms of weights, Annex A and Annex B tend to underestimate some parameters such as internal heat capacity by about 93% and 81%, attenuation by 85% and 86% and surface mass by 62% and 70%, especially in warmer climates such as Palermo.

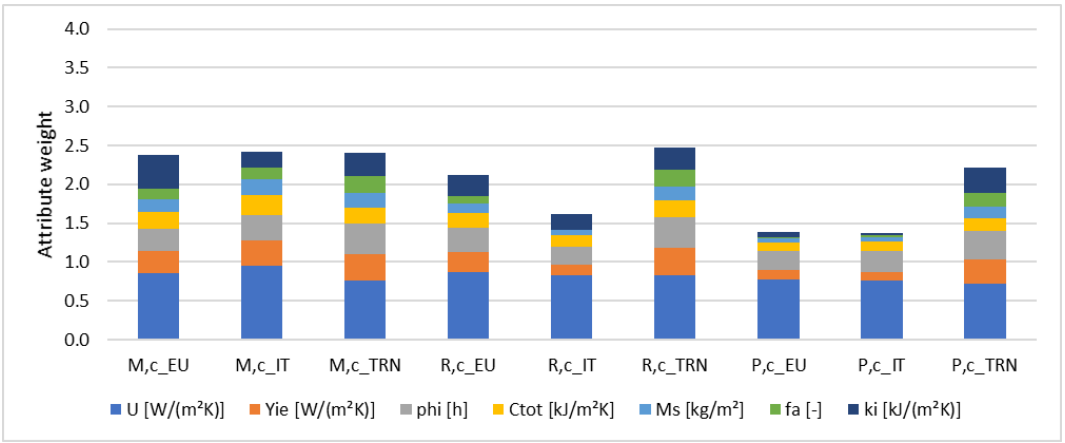

Figure 14. Weight analysis of the thermo-physical attributes of opaque structures, for the summer period and with $g_{gl,n}$ = 0.77.

The weights of the attributes calculated by Annex A and Annex B seem to have no more correspondence with the weights calculated by Trnsys if the solar transmission coefficient is set to 0.34. From Figure 15 it can be observed that the thermal transmittance, except for the city of Milan, is underestimated by both Annexes of EN ISO 52016-1. This leads to state that for particularly energy efficient structures in the summer period, where there is a strong dynamism of the boundary conditions, the method of EN ISO 52016-1 fails to correctly evaluate the weight of some parameters.

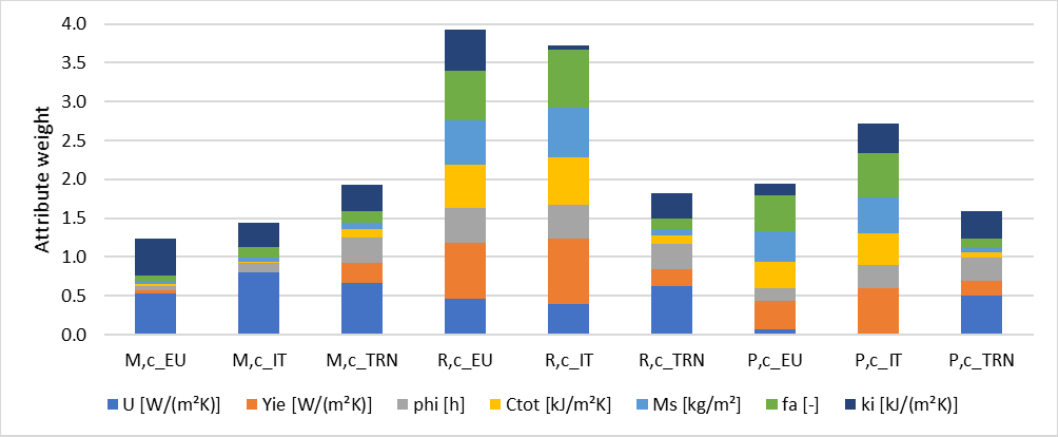

Figure 15. Weight analysis of the thermo-physical attributes of opaque structures, for the summer period and with $g_{gl,n}$ = 0.34.

5. Conclusions

A total of 1854 cases were analyzed using three different calculation methods, including the combination of 103 different stratigraphies, three climate zones and two solar transmission coefficients. These combinations produce low energy building solutions. Comparison between Trnsys results and those obtained from the two annexes of EN ISO 52016-1 showed that:

- The absolute error RMSE is extremely small. Both methods show variations of less than 1 kWh for heating, while for cooling the variations are less than 2 kWh (in the case of $g_{gl,n}$ = 0.77) and less than 2.2 kWh (in the case of $g_{gl,n}$ = 0.34). In absolute terms, Annex A performs better. This result is congruent with the comparative analysis carried out by Mazzarella et al. [12] between the two models of the Annexes and the analytical solution with sinusoidal boundary conditions. In all the test cases, the results obtained applying the Italian Annex provide better results, with a reduction of the error on the internal flow amplitude between 14% and 67% and an overestimation of the external flow amplitude compared to the analytical solution of 3%.
- The relative error CV(RMSE) is often over the 30% ASHRAE limit. It should be noted, however, that this is mainly caused by the low energy requirements of the analyzed solutions, which affect the denominator of the relative error formula. Only in the winter phase and for the coldest city the CV(RMSE) is verified. Specifically, for the case study with $g_{gl,n}$ = 0.77 the verification is satisfied for 16 cases (5.2%) with Annex B and for 45 cases (14.6%) with Annex A, while for the case study with $g_{gl,n}$ = 0.34, 51 cases (16.5%) with Annex B and 81 cases (26.2%) with Annex A. The contrast between the excellent results obtained in terms of RMSE and the low percentage of cases that satisfy the limit of 30% in terms of CV (RMSE) leads us to affirm that the verification proposed by ASHRAE to validate dynamic calculation methods, is not fully adequate in the case of low-energy buildings.
- In general, decreasing the g_{gl} (thus increasing the performance of the glazed structures) produces a higher RMSE. Indeed, a worse average error of 12.9% and 11.6% is obtained in the winter season for the method described in Annex B and Annex A, respectively, while 9.3% and 11.7% in the summer season. These results suggest that the EN ISO 52016-1 algorithm, regardless of the annex used, has an accuracy inversely proportional to the performance of the building: the lower the consumption, the greater the error committed with respect to the energy needs calculated by Trnsys.
- In terms of internal and surface temperatures, the RMSE of Annex B compared to Trnsys seems to vary according to the positioning of the mass inside the wall, with the worst result for the wall with external mass. For Annex A, the RMSE is approximately constant for each proposed solution. This allows us to state that the heat

transfer model of the opaque elements proposed in the European Annex (Annex B) favors some masonry types over others, in particular the one with distributed thermal mass. Overestimating the surface temperatures of the thermal zones implies an incorrect calculation of the operating temperature and consequently an incorrect energy requirement.

- Through a sensitivity analysis of the thermo-physical parameters of the walls, it can be stated that in the heating period the different calculation models are particularly aligned. In the summer period, on the other hand, the weights of the contributions are very variable for the different methods and the different case studies. In particular, for solar transmission coefficient equal to 0.34, the weights of the attributes calculated by Annex A and Annex B seem to have no correspondence with the weights calculated by Trnsys.
- Although ISO 52016-1 considers the angle of incidence of solar radiation, it overlooks that g_{gl} can vary considerably depending on the time of day and the day of the year. Implementing the Karlsson et al. method [16] within the general algorithm allows to improve the RMSE of summer solar loads by 46.7% compared to the method proposed by the standard. Improving the estimation of solar loads allows an improvement in the calculation of summer needs.

In conclusion, it can be stated that the method proposed in the Italian national annex and the Karlsson method for the calculation of solar contributions represent an improvement on the current EN ISO 52016-1. Future work will focus on the comparative analysis of the methods described in the two Annexes of EN ISO 52016-1 and the measurements collected in the field through an experimental mock-up.

Author Contributions: Conceptualization, S.S.; methodology, S.S. and G.R.; software, S.S. and G.R.; validation, S.S. and G.R.; formal analysis, S.S.; investigation, S.S.; resources, S.S. and G.R.; data curation, S.S.; writing—original draft preparation, S.S.; writing—review and editing, S.S. and G.R.; visualization, S.S. and C.D.P.; supervision, S.S. and C.D.P. All authors have read and agreed to the published version of the manuscript.

Funding: This research received no external funding.

Conflicts of Interest: The authors declare no conflict of interest.

Abbreviations

The following abbreviations are used in this manuscript:

U	Thermal transmittance	$W/(m^2K)$
M_s	Surface mass	kg/m^2
Y_{IE}	Periodic thermal transmittance	$W/(m^2K)$
f_a	Attenuation factor	-
φ/phi	Phase shift	h
κ_j	Internal areal heat capacity	$kJ/(m^2K)$
Ctot	Total heat capacity	$kJ/(m^2K)$
g_{gl}	Total solar energy trasmittance	-
$g_{gl,n}$	Total normal transmittance of solar energy	-
Fw	Exposition factor	-
$I_{sol,dir/dif,t}$	Direct/diffuse solar radiation incident on the glazed surface	W/m^2
$F_{sh,obst,t}$	Shading reduction factor	-
$\vartheta_{sol,t}$	Angle of incidence of direct solar radiation	°
p	Number of glass panels	-
q	Coefficient of glass coating type	-
θ_e	Outdoor temperature	°C
I_H	Horizontal solar radiation	W/m^2
HDD	Heating degree days	-

Appendix A. Specifications of the Opaque Structures Used

Table A1. Thermo-physical properties of all stratigraphies used for case study simulations.

N.	Distribution of Mass	U	M_s	Y_{IE}	f_a	φ	κ_j
-	-	W/(m^{2}K)	kg/m^2	W/(m^{2}K)	-	h	kJ/(m^{2}K)
1	D	0.228	315.00	0.004	0.019	23.10	44.12
2	D	0.315	246.00	0.019	0.060	18.75	37.60
3	D	0.343	294.00	0.018	0.052	18.18	44.02
4	D	0.230	432.00	0.001	0.005	5.93	39.57
5	D	0.355	228.00	0.026	0.074	16.83	39.10
6	D	0.368	353.20	0.013	0.036	20.83	41.74
7	D	0.356	274.85	0.018	0.050	18.55	40.55
8	D	0.237	228.86	0.007	0.031	21.10	35.77
9	D	0.218	227.80	0.007	0.031	21.92	34.56
10	D	0.163	292.99	0.001	0.006	29.22	34.36
11	D	0.238	265.09	0.006	0.026	22.70	36.17
12	D	0.243	444.15	0.002	0.010	26.95	38.85
13	D	0.208	444.15	0.001	0.004	29.08	38.86
14	D	0.343	375.06	0.011	0.033	20.35	41.30
15	D	0.209	360.00	0.001	0.005	28.72	41.93
16	D	0.215	287.00	0.003	0.015	25.35	39.77
17	D	0.169	369.00	0.001	0.003	32.77	39.80
18	D	0.192	328.00	0.001	0.007	28.88	39.87
19	D	0.239	308.25	0.004	0.017	24.57	37.29
20	D	0.310	404.10	0.005	0.016	24.70	41.48
21	D	0.230	432.00	0.001	0.005	5.93	39.57
22	D	0.215	52.13	0.120	0.554	6.67	21.63
23	D	0.244	49.63	0.154	0.631	5.87	22.12
24	D	0.364	44.18	0.288	0.793	4.31	22.79
25	D	0.281	47.93	0.191	0.679	5.50	22.24
26	D	0.383	43.55	0.310	0.810	4.13	22.66
27	D	0.292	47.30	0.204	0.699	5.30	22.38
28	D	0.271	48.55	0.179	0.660	5.70	22.22
29	D	0.371	199.50	0.048	0.130	13.80	44.38
30	D	0.296	265.60	0.013	0.044	20.20	37.73
31	D	0.285	345.60	0.006	0.020	23.76	39.50
32	D	0.262	187.60	0.020	0.075	17.86	34.47
33	D	0.380	246.75	0.040	0.105	15.40	38.84
34	D	0.275	270.00	0.007	0.027	21.40	41.82
35	D	0.352	180.00	0.036	0.102	15.08	41.94
36	D	0.363	164.00	0.059	0.163	14.21	39.97
37	D	0.252	246.00	0.009	0.035	21.50	39.74
38	D	0.402	196.00	0.059	0.146	13.08	44.58
39	D	0.518	246.75	0.090	0.173	12.90	42.23
40	D	0.482	41.05	0.422	0.875	3.20	22.12
41	IE	0.323	286.44	0.135	0.418	6.73	50.13
42	IE	0.233	278.64	0.056	0.241	10.70	42.74
43	IE	0.369	271.14	0.115	0.310	8.68	43.64
44	IE	0.226	20.55	0.192	0.888	3.81	34.26
45	IE	0.248	19.95	0.223	0.901	3.46	33.99
46	IE	0.350	18.75	0.321	0.918	2.88	33.20
47	IE	0.339	272.38	0.048	0.141	14.28	42.76
48	IE	0.266	276.13	0.033	0.125	15.30	42.52
49	IE	0.376	285.19	0.067	0.178	12.41	49.46
50	IE	0.295	285.94	0.050	0.169	12.80	49.37
51	IE	0.260	25.10	0.227	0.871	3.96	36.96

Table A1. *Cont.*

N.	Distribution of Mass	U	M_s	Y_{IE}	f_a	φ	κ_j
-	-	W/(m^{2}K)	kg/m^2	W/(m^{2}K)	-	h	kJ/(m^{2}K)
52	IE	0.303	19.20	0.276	0.913	3.08	33.53
53	IE	0.322	24.35	0.284	0.883	3.58	36.54
54	IE	0.368	18.60	0.339	0.920	2.83	33.08
55	IE	0.598	17.55	0.570	0.953	2.03	26.22
56	IE	0.561	14.98	0.528	0.941	2.22	30.39
57	I	0.259	249.13	0.008	0.031	20.56	37.70
58	I	0.269	248.50	0.009	0.034	20.36	37.69
59	I	0.253	229.50	0.010	0.041	17.90	39.16
60	I	0.298	228.90	0.015	0.051	17.50	39.13
61	I	0.326	228.60	0.020	0.061	17.20	39.11
62	I	0.278	354.10	0.004	0.015	22.81	41.87
63	I	0.317	353.65	0.006	0.020	22.33	41.83
64	I	0.255	381.31	0.004	0.016	21.68	41.89
65	I	0.264	380.69	0.005	0.018	21.53	41.39
66	I	0.284	379.44	0.006	0.021	21.25	41.37
67	I	0.287	238.60	0.035	0.121	12.30	45.99
68	I	0.328	238.15	0.042	0.128	12.10	46.10
69	I	0.383	237.70	0.053	0.138	11.90	46.25
70	I	0.262	404.70	0.002	0.007	2.36	41.51
71	I	0.208	253.50	0.004	0.020	21.68	37.76
72	I	0.207	230.40	0.007	0.033	18.35	39.18
73	I	0.197	355.60	0.002	0.009	23.60	41.90
74	I	0.211	385.06	0.003	0.014	22.55	41.41
75	I	0.227	405.30	0.001	0.005	26.85	41.52
76	I	0.214	239.80	0.023	0.109	12.88	45.83
77	I	0.345	238.00	0.045	0.131	12.03	46.14
78	I	0.580	236.80	0.109	0.187	11.32	47.08
79	I	0.462	237.25	0.071	0.154	11.67	46.52
80	I	0.505	196.25	0.121	0.239	9.67	47.52
81	E	0.208	253.50	0.005	0.022	21.45	23.47
82	E	0.207	230.40	0.008	0.039	18.03	21.56
83	E	0.197	355.60	0.002	0.011	23.26	21.57
84	E	0.211	385.06	0.003	0.016	22.26	23.58
85	E	0.214	239.80	0.030	0.139	12.51	21.94
86	E	0.345	238.00	0.056	0.163	11.65	22.01
87	E	0.227	405.30	0.001	0.006	2.53	22.33
88	E	0.259	249.13	0.009	0.033	20.33	25.14
89	E	0.269	248.50	0.010	0.036	20.13	26.10
90	E	0.274	229.20	0.014	0.052	17.40	22.27
91	E	0.298	228.90	0.017	0.058	17.18	23.17
92	E	0.278	354.10	0.005	0.017	22.46	23.19
93	E	0.317	353.65	0.007	0.022	22.00	26.93
94	E	0.255	381.31	0.005	0.020	21.36	23.31
95	E	0.264	380.69	0.006	0.022	21.21	23.40
96	E	0.284	379.44	0.007	0.024	20.93	23.87
97	E	0.321	377.56	0.010	0.031	20.41	26.16
98	E	0.328	238.15	0.052	0.159	11.71	21.91
99	E	0.383	237.70	0.065	0.170	11.50	22.33
100	E	0.262	404.70	0.002	0.008	2.05	25.21
101	E	0.538	199.28	0.135	0.251	10.77	29.74
102	E	0.442	201.15	0.090	0.205	11.35	25.41
103	E	0.417	201.78	0.081	0.195	11.50	24.77

Appendix B. Sensitivity Analysis of Thermo-Physical Parameters of Opaque Structures

Legend:

Range	Upper limit
0.000–0.150	0.150
0.151–0.300	0.150
0.301–0.450	0.450
0.451–0.600	0.600
0.601–0.750	0.600
0.751–0.900	0.900
0.901–1.000	1.000

Table A2. Weight analysis of the thermo-physical attributes of opaque structures, for the winter period and with g_{gl} = 0.77.

	M,h_EU	M,h_IT	M,h_TRN	R,h_EU	R,h_IT	R,h_TRN	P,h_EU	P,h_IT	P,h_TRN
U [W/(m^{2}K)]	0.999	0.996	0.997	0.998	0.992	0.994	0.979	0.985	0.974
Yie [W/(m^{2}K)]	0.564	0.567	0.576	0.565	0.526	0.580	0.585	0.604	0.592
phi [h]	0.468	0.454	0.479	0.470	0.444	0.484	0.477	0.479	0.500
Ctot [kJ/m^{2}K]	0.439	0.448	0.453	0.437	0.430	0.452	0.457	0.479	0.451
Ms [kg/m^2]	0.388	0.396	0.405	0.385	0.374	0.405	0.403	0.426	0.408
fa [-]	0.378	0.376	0.392	0.376	0.347	0.396	0.395	0.409	0.414
ki [kJ/(m^{2}K)]	0.053	0.030	0.077	0.028	0.038	0.082	0.099	0.041	0.102

Table A3. Weight analysis of the thermo-physical attributes of opaque structures, for the summer period and with g_{gl} = 0.77.

	M,c_EU	M,c_IT	M,c_TRN	R,c_EU	R,c_IT	R,c_TRN	P,c_EU	P,c_IT	P,c_TRN
U [W/(m^{2}K)]	0.852	0.954	0.762	0.876	0.833	0.825	0.775	0.759	0.727
Yie [W/(m^{2}K)]	0.291	0.322	0.345	0.253	0.127	0.352	0.123	0.116	0.303
phi [h]	0.290	0.325	0.385	0.310	0.243	0.394	0.244	0.273	0.365
Ctot [kJ/m^{2}K]	0.208	0.259	0.211	0.190	0.138	0.220	0.113	0.121	0.170
Ms [kg/m^2]	0.163	0.200	0.184	0.129	0.072	0.186	0.043	0.055	0.143
fa [-]	0.135	0.151	0.221	0.088	0.001	0.214	0.025	0.028	0.186
ki [kJ/(m^{2}K)]	0.439	0.203	0.302	0.273	0.206	0.288	0.061	0.022	0.320

Table A4. Weight analysis of the thermo-physical attributes of opaque structures, for the winter period and with g_{gl} = 0.34.

	M,h_EU	M,h_IT	M,h_TRN	R,h_EU	R,h_IT	R,h_TRN	P,h_EU	P,h_IT	P,h_TRN
U [W/(m^{2}K)]	0.998	0.996	0.996	0.999	0.995	0.993	0.988	0.993	0.970
Yie [W/(m^{2}K)]	0.552	0.556	0.566	0.551	0.553	0.568	0.556	0.572	0.566
phi [h]	0.463	0.447	0.473	0.459	0.445	0.477	0.467	0.454	0.488
Ctot [kJ/m^{2}K]	0.428	0.438	0.442	0.424	0.433	0.439	0.423	0.452	0.425
Ms [kg/m^2]	0.378	0.386	0.393	0.372	0.380	0.392	0.368	0.398	0.382
fa [-]	0.365	0.365	0.381	0.361	0.358	0.383	0.358	0.378	0.389
ki [kJ/(m^{2}K)]	0.092	0.042	0.085	0.061	0.025	0.095	0.033	0.037	0.129

Table A5. Weight analysis of the thermo-physical attributes of opaque structures, for the summer period and with g_{gl} = 0.34.

	M,c_EU	M,c_IT	M,c_TRN	R,c_EU	R,c_IT	R,c_TRN	P,c_EU	P,c_IT	P,c_TRN
U [W/(m^{2}K)]	0.537	0.798	0.670	0.461	0.394	0.619	0.064	0.014	0.510
Yie [W/(m^{2}K)]	0.036	0.001	0.254	0.724	0.843	0.227	0.375	0.588	0.188
phi [h]	0.050	0.131	0.324	0.446	0.440	0.318	0.153	0.300	0.294
Ctot [kJ/m^{2}K]	0.024	0.002	0.112	0.556	0.612	0.106	0.342	0.406	0.068
Ms [kg/m^2]	0.050	0.063	0.082	0.565	0.630	0.083	0.394	0.455	0.054
fa [-]	0.063	0.136	0.145	0.642	0.753	0.135	0.461	0.579	0.119
ki [kJ/(m^{2}K)]	0.481	0.312	0.341	0.531	0.055	0.334	0.149	0.376	0.357

References

1. European Commission, A Roadmap for Moving to a Competitive Low Carbon Economy in 2050, European Commission. 2011. Available online: https://www.gazzettaufficiale.it/eli/gu/1993/10/14/242/so/96/sg/pdf (accessed on 1 November 2021).
2. European Parliament, Energy. Topics: Energy Efficiency. Buildings, European Commission. 2018. Available online: https://eur-lex.europa.eu/legal-content/EN/TXT/PDF/?uri=CELEX:32018L0844&from=EN (accessed on 1 November 2021).
3. European Parliament. Directive (EU) 2018/844 of the European Parliament and of the Council of 30 May 2018 amending Directive 2010/31/EU on the energy performance of buildings and Directive 2012/27/EU on energy efficiency. *Off. J. Eur. Union.* **2018**, 75–91. [CrossRef]
4. *EN ISO 52016-1*; 2017—Energy Performance of Buildings—Energy Needs for Heating and Cooling, Internal Temperatures and Sensible and Latent Head Loads—Part 1: Calculation Procedures Performance. International Organization for Standardization: Geneva, Switzerland, 2017.
5. Zhang, H.; Shu, H. A Comprehensive Evaluation on Energy, Economic and Environmental Performance of the Trombe Wall during the Heating Season. *J. Therm. Sci.* **2019**, *28*, 1141–1149. [CrossRef]
6. Bagarić, M.; Pečur, I.B.; Milovanović, B. Hygrothermal performance of ventilated prefabricated sandwich wall panel from recycled construction and demolition waste—A case study. *Energy Build.* **2020**, *206*, 109573. [CrossRef]
7. Di Giuseppe, E.; Ulpiani, G.; Summa, S.; Tarabelli, L.; Di Perna, C.; D'Orazio, M. Hourly dynamic and monthly semi-stationary calculation methods applied to nZEBs: Impacts on energy and comfort. *IOP Conf. Ser. Mater. Sci. Eng.* **2019**, *609*, 072008. [CrossRef]
8. Congedo, P.M.; Baglivo, C.; Centonze, G. Walls comparative evaluation for the thermal performance improvement of low-rise residential buildings in warm Mediterranean climate. *J. Build. Eng.* **2020**, *28*, 101059. [CrossRef]
9. Ballarini, I.; Costantino, A.; Fabrizio, E.; Corrado, V. A Methodology to Investigate the Deviations between Simple and Detailed Dynamic Methods for the Building Energy Performance Assessment. *Energies* **2020**, *13*, 6217. [CrossRef]
10. Zakula, T.; Bagaric, M.; Ferdelji, N.; Milovanovic, B.; Mudrinic, S.; Ritosa, K. Comparison of dynamic simulations and the ISO 52016 standard for the assessment of building energy performance. *Appl. Energy* **2019**, *254*, 113553. [CrossRef]
11. Zakula, T.; Badun, N.; Ferdelji, N.; Ugrina, I. Framework for the ISO 52016 standard accuracy prediction based on the in-depth sensitivity analysis. *Appl. Energy* **2021**, *298*, 117089. [CrossRef]
12. Mazzarella, L.; Scoccia, R.; Colombo, P.; Motta, M. Improvement to EN ISO 52016-1:2017 hourly heat transfer through a wall assessment: The Italian National Annex. *Energy Build.* **2020**, *210*, 109758. [CrossRef]
13. Duffy, M.J.; Hiller, M.; Bradley, D.E.; Werner Keilholz, J.W. TRNSYS 17: A Transient System Simulation Program. 2013. Available online: https://sel.me.wisc.edu/trnsys/features/features.html (accessed on 1 November 2021).
14. CEN European Commitee for Standardization. *Indoor Environmental Input Parameters for Design and Assessment of Energy Performance of Buildings Addressing Indoor Air Quality, Thermal Environment, Lighting and Acoustics*; EN 15251; CEN: Brussels, Belgium, 2007.
15. Bergman, T.; Incropera, F.; DeWitt, D.; Lavine, A. *Fundamentals of Heat and Mass Transfer*, 7th ed.; Wiley: Hoboken, NJ, USA, 2011.
16. Karlsson, J.; Roos, A. Modelling the angular behaviour of the total solar energy transmittance of windows. *Sol. Energy* **2000**, *69*, 321–329. [CrossRef]
17. Shin, M.; Haberl, J.S. Thermal zoning for building HVAC design and energy simulation: A literature review. *Energy Build.* **2019**, *203*, 109429. [CrossRef]
18. Minister of Economic Development, Italian Ministerial Decree of 5th July 1975: Modification to the ministerial instructions dated 20th June 1896 concerning the minimal height and the main hygienic-sanitary requirements in housing units, 1975 (1975) 18–20.
19. *UNI 10840*; UNI-Ente Nazionale Italiano di Unificazione, 2007-Light and lighting-School rooms-General criteria for the artificial and natural lighting. UNI: Milan, Italy, 2007.
20. Presidente Della Repubblica, Decreto del Presidente Della Repubblica 26 Agosto 1993, n. 412, Italy. 1993. Available online: https://www.gazzettaufficiale.it/eli/id/1993/10/14/093G0451/sg (accessed on 1 November 2021).
21. *ISO 52010-1:2017*; International Organization for Standardization, Energy Performance of Buildings—External Climatic Conditions—Part 1: Conversion of Climatic Data for Energy Calculations. CEN: Brussels, Belgium, 2017.

22. Summa, S.; Tarabelli, L.; Di Perna, C. Evaluation of ISO 52010-1:2017 and proposal for an alternative calculation procedure. *Sol. Energy* **2021**, *218*, 262–281. [CrossRef]
23. Meteotest, Meteonorm 7 V7.3.3, Bern, Switzerland. 2018. Available online: https://meteonorm.com/en/ (accessed on 1 November 2021).
24. Uni-Ente Nazionale Italiano Di Unificazione, Uni/Ts 11300-1:2014—Energy Performance of Buildings—Part 1: Evaluation of Energy Need for Space Heating and Cooling, Italy. 2014. Available online: http://store.uni.com/catalogo/norme/root-categorie-tc/uni/uni-ct-202/uni-ts-11300-1-2014?___store=en&___from_store=it (accessed on 1 November 2021).
25. Recurve, Support Articles (FAQs), (n.d.). Available online: https://www.recurve.com/support-articles/what-is-a-cvrmse-value (accessed on 1 November 2021).
26. ASHRAE Guideline 14, Measurement of Energy, Demand, and Water Savings. 2014. Available online: https://www.ashrae.org (accessed on 1 November 2021).
27. Willmott, C.J.; Matsuura, K. On the use of dimensioned measures of error to evaluate the performance of spatial interpolators. *Int. J. Geogr. Inf. Sci.* **2006**, *20*, 89–102. [CrossRef]
28. Moldovan, M.; Visa, I.; Neagoe, M.; Burduhos, B.G. Solar Heating & Cooling Energy Mixes to Transform Low Energy Buildings in Nearly Zero Energy Buildings. *Energy Procedia* **2014**, *48*, 924–937. [CrossRef]
29. Yıldız, Y.; Arsan, Z.D. Identification of the building parameters that influence heating and cooling energy loads for apartment buildings in hot-humid climates. *Energy* **2011**, *36*, 4287–4296. [CrossRef]
30. Li, H.; Wang, S.; Cheung, H. Sensitivity analysis of design parameters and optimal design for zero/low energy buildings in subtropical regions. *Appl. Energy* **2018**, *228*, 1280–1291. [CrossRef]
31. Zhao, M.; Künzel, H.M.; Antretter, F. Parameters influencing the energy performance of residential buildings in different Chinese climate zones. *Energy Build.* **2015**, *96*, 64–75. [CrossRef]
32. Mechri, H.E.; Capozzoli, A.; Corrado, V. USE of the ANOVA approach for sensitive building energy design. *Appl. Energy* **2010**, *87*, 3073–3083. [CrossRef]
33. Rapidminer. Available online: https://rapidminer.com (accessed on 1 November 2021).